

J. Electroanal. Chem., 319 (1991) 161–175
Elsevier Sequoia S.A., Lausanne
JEC 01768

Elevated-temperature excess heat production in a Pd + D system

Bor Yann Liaw * and Peng-Long Tao

Hawaii Natural Energy Institute, University of Hawaii, Holmes Hall 246, 2540 Dole Street, Honolulu, HI 96822 (USA)

Patrick Turner and Bruce E. Liebert

Department of Mechanical Engineering, University of Hawaii at Manoa, 2540 Dole Street, Honolulu, HI 96822 (USA)

(Received 26 March 1991; in revised form 30 July 1991)

Abstract

We report a new approach using a Pd|eutectic LiCl+KCl molten salt saturated with excess LiD|Al electrochemical cell to generate excess heat at elevated temperatures. For future utility applications, high-grade heat and high efficiencies can be expected from this novel process when it is operating above 350°C with its faster kinetics, compared with recent room-temperature aqueous-system operations. The electrolyte provides a very reducing environment, which offers the possibility of using less expensive non-noble-metal materials. A modified isoperibol calorimeter was used for the excess heat measurements. Preliminary results show high levels of excess heat output, although the effect remains sporadic. The Pd electrode shows a significant surface microstructural transformation after electrolysis. A small number of α -particles were found in the deuterated Pd electrode.

INTRODUCTION

The production of excess heat in a Pd + D system at ambient temperatures, as reported by Fleischmann et al. [1], suggested the possible emergence of a nearly inexhaustible, clean and inexpensive source of energy. Although many negative results have been reported (e.g. refs. 2, 3), increasing numbers of positive results have also been reported [4–8] in the detection of excess heat, tritium and neutrons, either separately or collectively, despite the fact that the nature of this reaction has not yet been conclusively identified.

* To whom correspondence should be addressed.

For practical purposes, the use of aqueous electrolytes in most of these studies has limited the employment of this technology to relatively low temperatures, typically below 100°C, unless a pressurized cell is used. The use of an elevated temperature approach, however, would hold an obvious advantage: in terms of thermodynamics and kinetics, the efficiency of electricity conversion and the diffusion of deuterium in palladium can both be increased.

It has been suggested [1] that high deuterium activity in palladium deuteride is critical to achieving excess power and heat. It is also known from the Pd-H phase diagram [9] that, at the same H/Pd ratio, the hydrogen partial pressure as well as the deuterium activity in metal deuterides increase quite significantly with temperature.

The use of molten-salt electrochemical techniques to generate excess power and heat at elevated temperatures, typically above 350°C, is presented here. The use of molten-salt techniques to study metal-hydrogen systems was recently illustrated by Luedecke et al. [10,11] and by Liaw and coworkers [12,13], while the underlying principles were explicitly described by Deublein and Huggins [14]. The molten-salt electrolyte in this study is a eutectic LiCl + KCl mixture saturated with excess LiD, which has a melting temperature of about 350°C. LiD provides the deuteride-conducting species, D^- ions, in the electrolyte, along with a very strong reducing environment that removes surface oxides on metals and thus facilitates deuterium reaction with the metal. Many transition metals and their alloys [15,16], which can absorb substantial amounts of deuterium, often suffer from an impeding oxide surface layer in aqueous systems. Therefore these transition metals can be utilized in this molten-salt environment. Since quite a considerable amount of LiD can be incorporated into the melt, the electrolyte has a high ionic conductivity for D^- ions. Accordingly, we believe that this approach is superior to the aqueous system for producing excess heat in metals for many reasons, including operation at elevated temperatures to ensure higher thermodynamic efficiency, use of less expensive materials and, possibly, a higher gain in power through better kinetics.

PRINCIPLES

Recently, Deublein and Huggins [14] proposed a novel approach using a eutectic LiCl + KCl molten salt, saturated with LiH, as an effective means of preparing hydrogen-transparent metal surfaces. The same technique, demonstrated by Liaw and coworkers [12,13] and by Deublein et al. [17-19], showed that a strongly reducing hydride-conducting electrolyte could be used to control metal-hydrogen reactions in electrochemical cells. The alkali hydride used in the electrolyte dissociates in the melt and forms alkali and hydride ions. The hydride ion can thus be readily transported in the electrolyte and metal hydrides are produced electrochemically.

We expect the deuterium system to behave in a similar fashion. Therefore an electrochemically induced reaction, similar in nature to that reported by Fleisch-

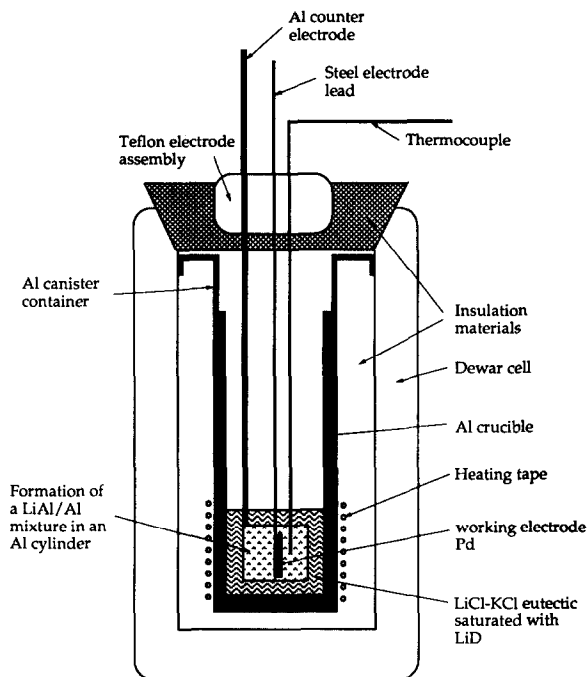
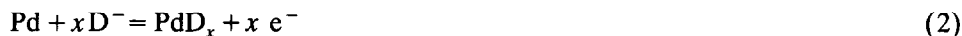


Fig. 1. Schematic drawing of the elevated-temperature molten-salt electrochemical cell.

mann et al. [1], can be conducted using a cell as shown in Fig. 1. The cell half-reactions are



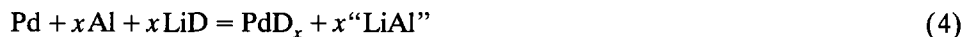
at the anode



at the cathode



which give the total cell reaction



with an endothermic reaction enthalpy ΔH_r estimated to be approximately 3 kJ mol^{-1} at 700 K^* . At this temperature, the palladium hydride and palladium deuteride are in the single α -phase region, above the α - β two-phase immiscibility regime [5]. In reaction (3), the Al is best described as the end composition of the

* Owing to lack of the formation enthalpy data for palladium deuteride at elevated temperatures, the reaction enthalpy was estimated from that at 298 K in Table 3.

α -Al phase and "LiAl", denotes the initial composition of the β -phase at the corresponding temperature [20].

The dynamic heat balance of the cell was periodically monitored by a thermocouple in an isoperibol calorimeter. The heat balance during electrolysis resulted in a change in the e.m.f. of the thermocouple and the resulting output power was subsequently determined from calibration data on the correspondence between power and the equilibrium thermocouple response.

EXPERIMENTAL ASPECTS

The cell shown in Fig. 1 consists of an Al container, an Al crucible and a Dewar flask densely packed with glass fiber (Kaowool, 8# density) insulation. Two Pd samples (Engelhard, 4 mm diameter wire, 99.99%) were torch-melted with a propane + oxygen flame. One of them, which weighed 0.4874 g before use, was wound with a molybdenum wire (Alfa Products, 0.127 mm diameter) to a current collector and used as the positive electrode (anode). The other was later used as a blank. A section of Al tubing (700/SF 6061), 2.54 cm long and 0.32 cm thick, was used as the negative electrode (cathode) to react with Li. The Al electrode was periodically replaced after being substantially loaded with Li. For the best result, the Al electrode was discarded after the composition passed the α - β two-phase region. Both current collectors were steel rods 0.3 cm in diameter. A high-temperature glass-fiber-insulated heating tape surrounding the lower portion of the container was the heat source for maintaining the cell temperature above 350°C. The power to the heating tape was maintained by a Novatron DCR 80-10 DC power supply (max. ± 80 V, 10 A; Sorensen/Raytheon Co., South Nowark, CT). The power could easily be maintained at a level of 50–80 W with a variation within 0.1 W. It should be noted that the power to the heating tape was kept constant throughout each experiment and the temperature of the cell was recorded before calorimetric work was performed.

Eutectic LiCl + KCl (47.6 wt.% KCl + 51.9 wt.% LiCl) was prepared by the Lithium Corporation of America and used as received. The eutectic melt (about 20 cm³) was heated inside the crucible for at least 1 day before 3–5 g LiD (Aldrich, 98 + at.% D) was added. This process helped to reduce the initial consumption of LiD by the moisture contaminant in the melt. The experiments were carried out in a controlled argon-filled glove-box in which oxygen and moisture were continuously removed.

The calorimetric measurements were based on a dynamic heat balance determined by a K-type thermocouple (chromel/alumel couple; Omega Engineering Inc.) in the electrolyte. The thermocouple was shielded with an ungrounded stainless steel sheath 0.1 cm in diameter. Because there was a large mass of metallic parts in the system, their conductive properties aided in the thermal equilibration of the dynamic heat balance. The ionic melt also conducts heat effectively. On the basis of this preliminary study, we believe that any local heating problem is considerably reduced with this approach.

The calibration procedure was conducted by employing the resistor heating tape, which was in contact with the reaction cell container, as a joule heat source. By varying the power P_r to the resistor heating tape we obtained a corresponding ΔT versus P_r relation as a calibration curve. The time constant of the calorimeter was in the range of 5–6 h, which was the time corresponding to imposing a power step on the system and the subsequent thermal equilibrium. An interval of at least 12 h separated each calibration step. It should be noted that all the temperature values ΔT reported in this paper correspond to the difference between the cell temperature represented by the thermocouple reading and the ambient temperature of the glove-box, which was maintained between 25 and 30°C and constantly monitored by a thermometer inside the box. The calibration curve obtained after the high-current excursion was used in the interpretation of calorimetric data.

Two separate calorimetric experiments based on the Pd + D system were conducted. The Pd sample had an irregular shape due to melting with a surface area estimated to be about 0.99 cm². It was charged for more than 3 weeks at 4 mA cm⁻² to ensure complete loading of deuterium throughout the sample before later use for high-current excursions. After this precharging period, additional LiD was added and another short period of charging at a low current density was performed before switching to high current density charging. This ensured a high loading state for each experiment. All electrochemical work was performed with an EG & G Princeton Applied Research PARC-173 potentiostat/galvanostat under galvanostatic operation.

Scanning electron microscopy (SEM) (ISI Model SX-40A with a Princeton Gamma Technology energy-dispersive X-ray (EDX) elemental analysis system) was used to examine the morphology of the Pd samples. The difference in morphology between the deuterated sample and the blank is described below.

RESULTS

Figure 2 shows the time-dependent temperature excursion of the PdD_x/eutectic LiCl + KCl molten salt saturated with excess LiD/Al cell subjected to three high-current-density charging experiments. After 88 h of charging at 2.5 mA cm⁻², the current density was raised to 290 mA cm⁻² and a subsequent temperature rise was recorded. It took more than 6 h to reach a relatively steady temperature of 407°C, a 30°C increase from an electrochemical power input of only about 0.36 W. About 25 h later, the current density was increased to 420 mA cm⁻², which corresponds to an input electrochemical power of 0.92 W, and the temperature increased to 419°C. Another 47 h later, the current density was increased to 692 mA cm⁻², for an input electrochemical power of 1.68 W, and the resulting temperature was 460°C. A larger fluctuation in temperature was observed at this stage, which ended after 26.8 h, presumably because the LiD was exhausted. The cell returned to its initial rest temperature about 6 h after the termination of the input electrochemical power. This demonstrated that the thermocouple was functioning normally; no degradation of the thermocouple was observed.

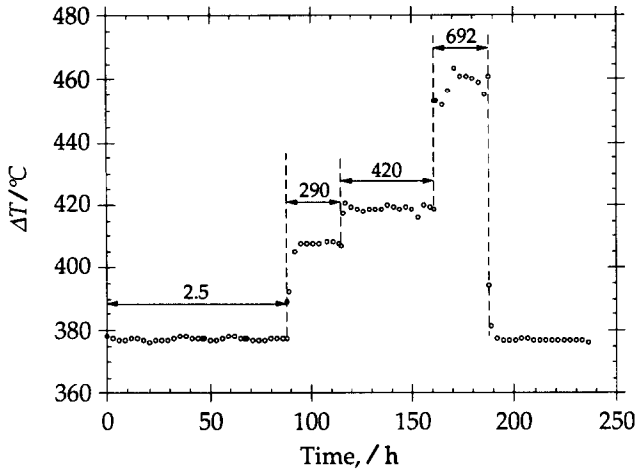


Fig. 2. Temperature variation during high-current-density charging experiments in the Pd+D system. The numbers are the charging current densities in mA cm^{-2} .

Figure 3 shows the results from the above experiments and another one charged at 606 mA cm^{-2} . Two calibration curves and the corresponding temperature response of the PdD_x /eutectic LiCl+KCl molten salt saturated with excess

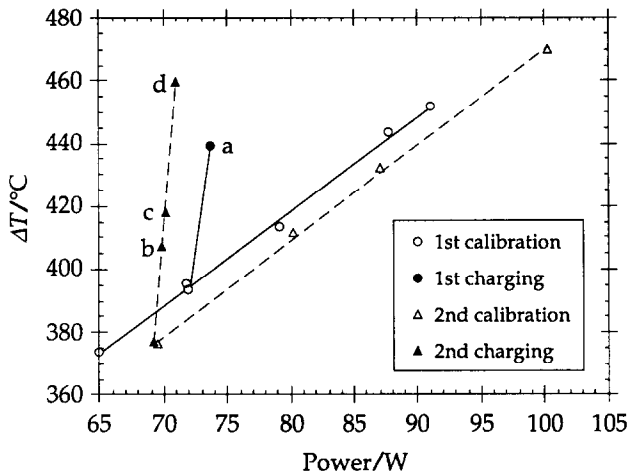


Fig. 3. Power balances during calibrations and high-current-density charging experiments. The calibration curves were obtained after each charging experiment and indicate the total input power-temperature relationships of the cell. The data from the charging experiments show that the temperature increases due to the total input power exceed what would be expected from the calibration curves. The charging current densities (mA cm^{-2}) were as follows: curve a, 606; curve b, 290; curve c, 420; curve d, 692.

TABLE 1

Parameters and power balances in the Pd + D experiments

Cell voltage /V	Current density /mA cm ⁻²	Power to heating tape, P_r /W	Electrochemical power /W	Total input power /W	Power output measured /W	Excess power /W	Excess power gain /%	Excess heat /MJ mol ⁻¹ D ₂
3.230	606	71.91	1.94	73.85	86.76	12.91	665	-4.15
2.188	290	69.25	0.63	69.88	79.24	9.36	1486	-6.27
2.270	420	69.30	0.94	70.24	82.81	12.57	1337	-5.83
2.453	692	69.25	1.68	70.93	96.34	25.41	1512	-7.16

LiD|Al cell under four different charging current densities are shown, with the values given in Table 1 for the measured cell voltage, current density, input heating power, input electrochemical power and output power, as well as the calculated excess power and heat. The total input power is the sum of the power supplied to the resistor heating tape and the electrochemical work applied to the cell, i.e. the product $E_c I$ of cell potential and current. Although the cell was an open system, the thermoneutral potential of the total cell reaction was not considered in the calculation of the input electrochemical power, which is therefore overestimated.

On the basis of the calibration data, we can convert the temperature reading into a measurable output power, as depicted in Fig. 4 for the experiments shown in Fig. 2. The difference between the measured output power and the total input power

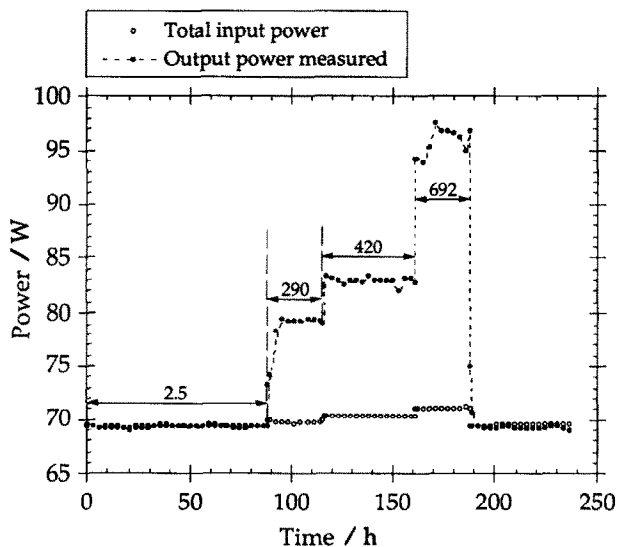


Fig. 4. Comparison of the input and output power of the Pd + D system during the high-current-density charging experiments. The numbers are the charging current densities in mA cm⁻².

power represents the excess power from the reaction. The area between the two curves is therefore the excess energy that was produced during the high-current-density charging experiments. Integration of the curves yields an excess energy of 5.02 MJ for this particular set of experiments, which was limited by the amount of LiD present in the cell. The electrochemical charge applied to the cell during the charging period was about 154 600 C, which corresponds to 0.801 mol of D_2 gas. Thus an excess heat of $6.26 \text{ MJ (mol } D_2)^{-1}$, or $1096 \text{ MJ (mol Pd)}^{-1}$, was obtained. This number is comparable with the number derived from the steady-state values, as shown in the last column of Table 1.

The magnitude of power and energy measured in these experiments was surprisingly high, as shown by the last entry in Table 1. The input power to the heating tape was maintained at about 69.25 W, the cell potential was typically in the range of 2.45 V, and the input electrochemical power was about 1.68 W at 692 mA cm^{-2} , which corresponds to a total input power of about 70.9 W. On the basis of the calibration curve, we would expect the 1.68 W of joule heating to result in a 5.1°C increase in temperature; however, the temperature increased by 82.4°C . In other words, this temperature rise corresponds to a power level of about 27.1 W, according to the calibration curve. Therefore a net gain of 25.4 W was in excess, which resulted in an excess power gain of 1512%, in the range of $627 \text{ W (cm}^3 \text{ Pd)}^{-1}$.

The surface morphology of the Pd samples is shown in Fig. 5. Figures 5(a) and 5(b) are of the blank Pd sample that did not experience electrolysis, while Figs. 5(c)–5(e) are of the Pd sample that was deuterated during the high-current excursion experiments. EDX results on the deuterated sample indicated some Fe and Zn contamination after electrolysis, as shown in Fig. 6(a). These contaminants were not detected by EDX in the blank (Fig. 6(b)).

Figure 7 shows the polarization behavior of a Pd deuteride | eutectic LiCl + KCl molten salt with excess LiD | "LiAl" / Al cell at 380°C . Values from four separate runs all fall on one curve ranging from 4 to 128 mA. The curve exhibits two distinguishing features: a logarithmic rise of potential with current in the low-current regime ($< 10 \text{ mA}$) and a steady linear increase of potential with current at higher currents ($> 10 \text{ mA}$).

DISCUSSION

Electrochemical aspects

Given the cell configuration Pd | eutectic LiCl + KCl molten salt saturated with excess LiD | Al, reactions (1)–(4) are considered to be predominant. The solubility of LiD in the eutectic LiCl + KCl mixture has not been measured quantitatively as yet. However, our physical examinations indicated that not all LiD ($> 3 \text{ g}$) dissolved in the melt (ca. 35–40 g). We assumed the dissociation constant of reaction (1) to be significant, as reflected by the high deuteride ionic conductivity of the melt. Nevertheless, the degree of dissociation of LiD in the melt has to be

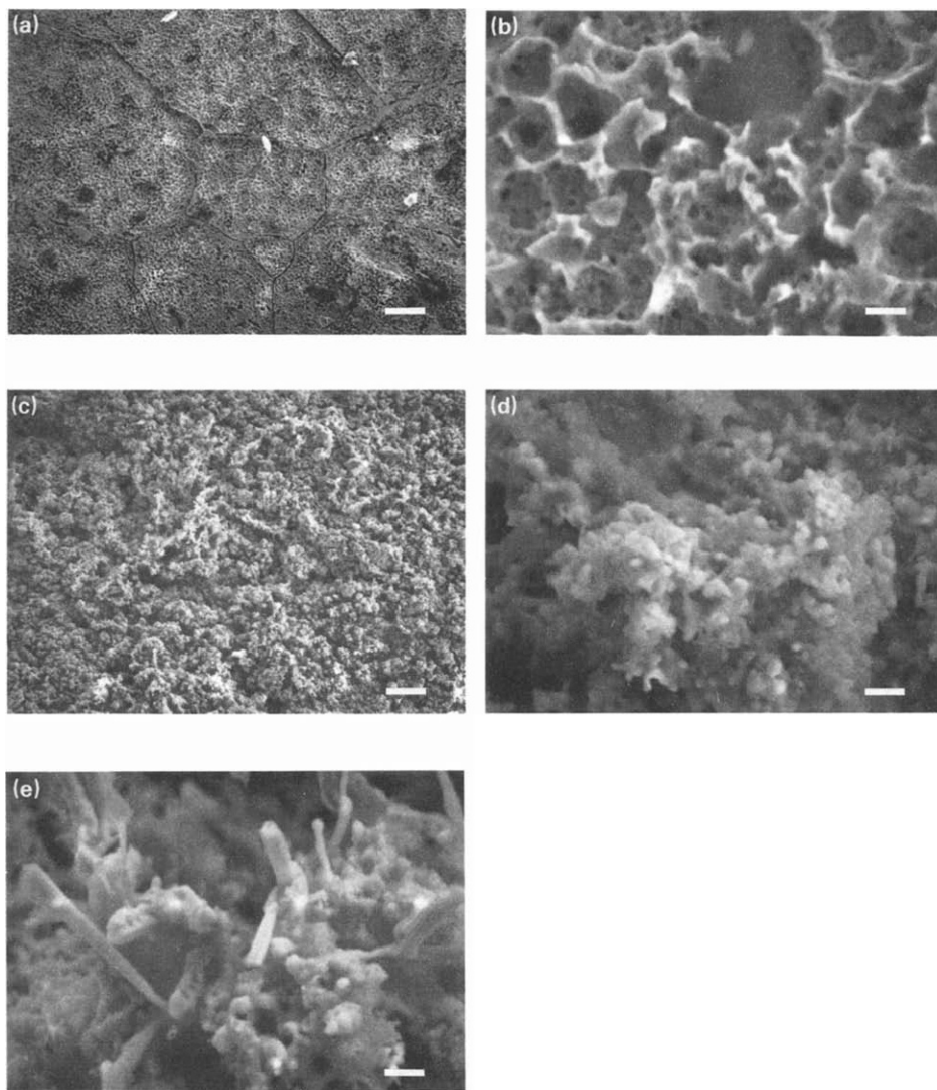


Fig. 5. (a) Low magnification SEM topography of a blank Pd sample that has been torch-melted. Grain boundary features are readily recognized as well as the high density of pores within the grains. (b) High magnification view of the surface porous ruffle-structure on the blank Pd sample. (c) Change in surface morphology after high-current-density deuterium charging experiments with no evidence of pre-existing grain structure. (d), (e) Cauliflower-structure formation of Pd codeposited layer accompanied by needle-like crystalline Pd-whisker precipitates. The white bar in the right lower corner on each figure represents (a) 40 μm , (b) 2 μm , (c) 40 μm , (d) 2 μm and (e) 2 μm .

studied more carefully. However, because of the amphoteric nature of the H(D) species, we prefer using a weak electrolyte model to describe this behavior.

The Gibbs energy of formation for LiH is reported to be $-39.83 \text{ kJ mol}^{-1}$ at

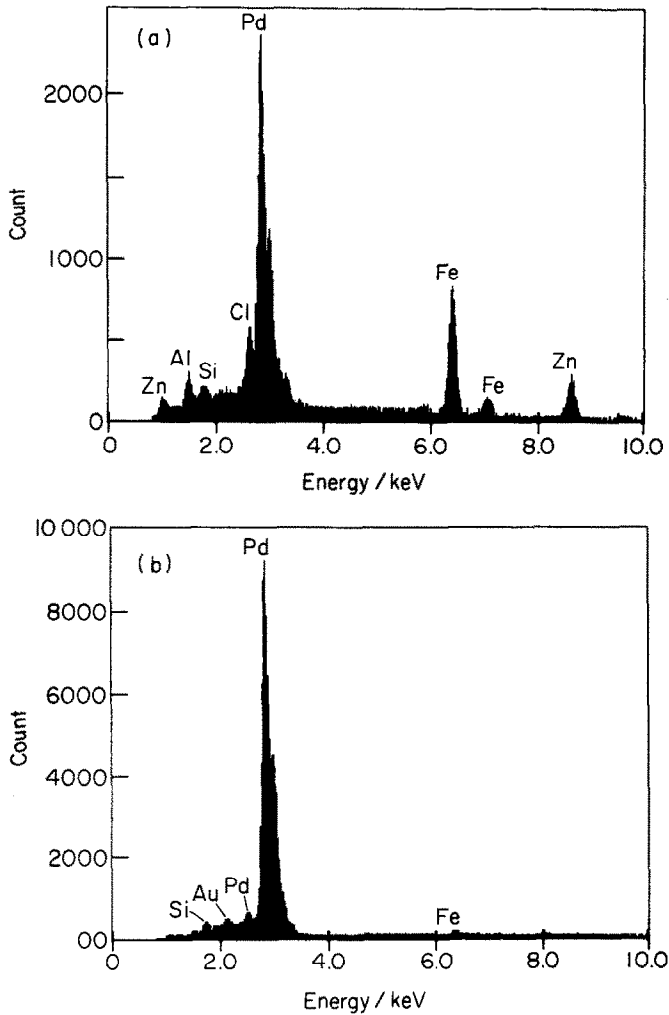


Fig. 6. EDX elemental analysis of (a) the Pd sample after the high-current-density deuterium charging experiments (averaged over the area shown in Fig. 5(c)) and (b) the blank. In (a), Fe and Zn were identified as minute contaminants, possibly arising from the cell components.

653 K (380°C) [21]. This corresponds to a 412.7 mV span, i.e. a standard hydrogen reversible electrode in the hydride electrolyte environment is 412.7 mV above the standard reversible lithium electrode. Considering that the “LiAl”/Al reference potential is 307.3 mV above the standard reversible lithium electrode [22,23] at 653 K, we estimate that the reversible hydrogen evolution reaction should occur at 105.4 mV above the reference electrode. Therefore, this potential is the reversible cell potential for a PdH_x (where $a_{\text{H}} = 1$)|eutectic LiCl + KCl with excess LiH|“LiAl”/Al cell. The potential for the deuterium system should be very

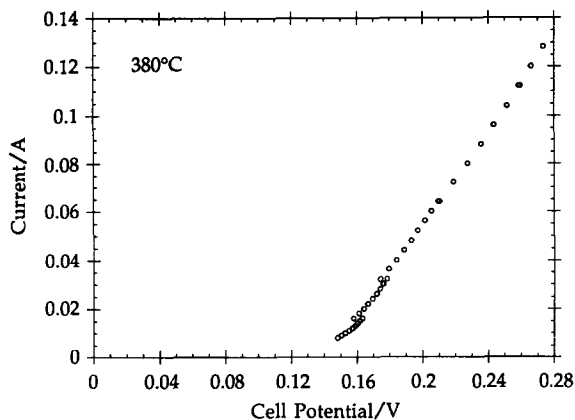


Fig. 7. Polarization behavior for a PdD_x | eutectic $\text{LiCl} + \text{KCl}$ molten salt with excess LiD | “ LiAl ” / Al cell at 380°C .

similar and slightly higher (Fig. 7). The similarity between the thermodynamic calculation and experimental result indicates that the reaction



requires an energy close to the Gibbs energy of decomposition of LiD ,



i.e. 40.5 kJ mol^{-1} , as estimated from LiH . Therefore, the Gibbs energy of dissociation for reaction (1) is likely to be negligible. Because LiD is considered to be a weak electrolyte in the pure ionic chloride melt, the associated dissolution entropy change is expected to be small. We believe that the enthalpy change for reaction (1) is small as well.

Our experimental conditions indicated that, owing to the limited solubility of LiD in the melt, the electrolysis proceeded with both dissolution and dissociation of LiD in the electrolyte and reduction/oxidation of the respective ion on the electrodes.

The reaction of the Al cathode with Li in similar molten salt environments has been intensively studied in many laboratories (e.g. refs. 22 and 23). A recent review of the $\text{Li} + \text{Al}$ binary system was given by Chen et al. [20]. The reaction of Li with Al is very fast at high temperatures and the phase transformation proceeds at high rates. The two-phase mixture of “ LiAl ” and Al exhibits a constant potential plateau, as described in refs. 22 and 23, which serves as an internal reference.

Thermochemical aspects

Most of the thermodynamic data, especially the enthalpies, which represent heat associated with the formation of compounds and the solution of hydrogen in

TABLE 2

Enthalpies of compounds involved in the Pd + D systems at 298 and 700 K ^a

Compounds	ΔH at 298 K /kJ mol ⁻¹	ΔH at 700 K /kJ mol ⁻¹
LiH	-90.60	-94.695
LiD	-90.90 ^b	
LiCl	-408.169	-408.491
KCl	-436.58	-436.54
PdCl ₂	-173.13	-166.47
LiAl	-48.94	-53.237
PdH _x (β hydride formation)	-11.21 ($x = 0.56$, 303 K) ^c	
dissolution	-37.23 (in metal, 303 K) ^c	-39.3 ($x = 0.35$) ^d
		-11.7 ($x = 0.65$) ^d
PdD _x (β deuteride formation)	-9.83 ($x = 0.56$, 303 K) ^c	

^a Data from ref. 21.^b From CRC Handbook of Chemistry and Physics, 65th edition, R.C. Weast and M.J. Astle (Eds.), CRC Press, Boca Raton, FL, 1984-85.^c Data from G.G. Libowitz, The Solid State Chemistry of Binary Metal Hydrides, Benjamin, New York, 1965.^d ΔH decreases in magnitude with increasing H/Pd. Data from ref. 9.

the system, can be found in the literature [21]. When all reactions that are known to occur in the system are considered, no reason can be found that would justify attributing the excess power generation to a thermochemical reaction. Thus these results suggest that the effect is non-chemical.

The reported enthalpies of the compounds associated with this system are compiled in Table 2. Table 3 lists possible chemical reactions and their corre-

TABLE 3

Calculated enthalpies of reaction in the Pd + D system at 298 and 700 K

Reaction	ΔH_r at 298 K /kJ mol ⁻¹	ΔH_r at 700 K /kJ mol ⁻¹
0.56LiH + Pd + 0.56Al \rightleftharpoons 0.56LiAl + PdH _{0.56} (hydride formation)	12.13	
0.56 LiD + Pd + 0.56 Al \rightleftharpoons 0.56 LiAl + PdD _{0.56} (deuteride formation)	13.68	
δ LiH + PdH _x + δ Al \rightleftharpoons δ LiAl + PdH _{x+\delta} (hydrogen dissolution)	23.05	2.13 ($x = 0.35$) 29.74 ($x = 0.65$)
LiH + Al \rightleftharpoons LiAl + 1/2H ₂	41.66	41.45
LiD + Al \rightleftharpoons LiAl + 1/2D ₂	41.95	
2LiCl + PdH + 2Al \rightleftharpoons 2LiAl + PdCl ₂ + 1/2H ₂	556.55	
2LiCl + PdD + 2Al \rightleftharpoons 2LiAl + PdCl ₂ + 1/2D ₂	555.17	

sponding reaction enthalpies, as calculated from Table 2. All calculated enthalpies are positive for every possible reaction involving hydride or deuteride formation, hydrogen dissolution, gas evolution and chloride formation; consequently, these reactions are endothermic in nature and should not contribute to any excess power or heat measured.

Therefore the origin of the excess heat generation can only be attributed to a nuclear process, or maybe several processes, which are as yet unknown. There is increasing evidence [4–8] from other laboratories that tritium and neutrons have been detected in deuterated metals, which directly supports the hypothesis of a nuclear phenomenon. Our recent He analysis [24] of the two samples showed that ^4He was significantly above the background in the deuterated Pd sample but not in the blank. The detection of ^4He in the effluent gas from the electrolysis cells that gave excess heat, as reported by Bush et al. [25], is further evidence of a nuclear phenomenon. However, it seems that the phenomena are different from and far more complicated than those known to occur under high-temperature high-energy conditions using physical confinement methods.

Preliminary experiments based on LiH have been performed and will be discussed elsewhere [26]; however, no excess heat has been found in that system to date, which suggests that there is indeed a difference between the deuterium and hydrogen systems. The calorimetry results from the Pd + H system also agree with what would be expected from thermochemical reactions, verifying the correct response from the calorimetry techniques.

Morphological aspects

An intriguing feature of the SEM studies is the large extent of porous rough structure found on both as-prepared and electrolyzed sample surfaces. These porous features were introduced by torch melting, resulting in a grain and pore size typically in the range 300–500 μm (Fig. 5(a)) and 3–5 μm (Fig. 5(b)) respectively. The deuterated sample shows a larger pore-size distribution in the range 10–50 μm and sometimes up to hundreds of microns. There is no evidence of any grain structure in the deuterated sample.

It is known that Pd is quite ductile but becomes brittle after hydriding. We often found that portions of highly deuterided or hydrided samples were easily broken into pieces. The ruffle-like surface morphology of the non-deuterated sample (Fig. 5(b)) suggests that the formation of the pores resulted from the following process. A considerable amount of gas (primarily CO_2 and H_2O) was introduced and forced into the molten Pd by the torch flame. The gas formed highly dispersed bubbles in the molten Pd. Upon solidification, the gas bubbles near the surface were forced out and escaped at the surface, leaving porous channels and rugged ruffle-like thin walls on the Pd surface.

The dramatic morphology change by electrolysis is evidenced by the comparison of Figs. 5(c)–5(e) with Figs. 5(a) and 5(b). The much rougher surface shown in Fig. 5(c) implies that a new layer has been formed during electrolysis with evidence of a

“cauliflower-like” morphology (Fig. 5(d)). This new surface is predominantly Pd, according to EDX results (Fig. 6(a)). We suspect that high-current-charging excursions resulted in this “cauliflower-like” morphology formation in parallel with the deuterium transport. Quite possibly, the electrochemical deuterizing process at high potentials had a parallel process that caused substantial Pd dissolution (possibly by means of chloriding as PdCl_4^{2-}) and codeposition of a new Pd layer, which resulted in the microstructural rearrangement. In some locations, a needle-like crystalline phase was found and was identified by EDX to be Pd whiskers, as shown in Fig. 5(e).

The presence of Fe and Zn cannot be quantified from the EDX results (Fig. 6(a)). The Fe contaminants probably came from the steel current collectors. The Zn contaminant was probably from the Al electrode (since 6061 Al alloys contain 0.25% Zn). Whether these contaminants promote excess heat production is unknown; however, it is unlikely that either their presence and associated chemical reactions or the Pd dissolution/codeposition process would be the source of excess heat, simply because the amounts involved are far too small to be accounted for by the energy that was measured.

The significance of the morphology change of the Pd electrode to the production of excess heat is not known at this time. But the interesting features that we discovered in this experiment, along with our failure to reproduce excess heat using untreated Pd wires in the presence of macro- and micro-cracks, suggest that the interplay of surface morphology, microstructures and deuterium insertion into Pd may be of paramount importance in generating excess heat.

CONCLUSIONS

We have demonstrated that, employing novel molten-salt electrochemical techniques, excess power production was found in the Pd + D system. In one particular case, a large amount of excess heat ($6.26 \text{ MJ (mol D}_2\text{)}^{-1}$) was measured in a Pd + D charging experiment. The morphology of the Pd electrode may have a significant impact on excess heat production. Control of morphology of the Pd electrode and the production of excess heat have been difficult to replicate.

ACKNOWLEDGEMENTS

We would like to thank the University of Hawaii and the Pacific International Center for High Technology Research for financial support, Dr. S.K. Sharma for providing the Pd sample materials, Professor C.M. Jensen for allowing us to use the glove-box facility and Professor J.P. Cowen for permitting us the use of the SEM-EDX facilities.

REFERENCES

- 1 M. Fleischmann, S. Pons and M. Hawkins. *J. Electroanal. Chem.*, 261 (1989) 301; Err., 263 (1989) 187.

- 2 N.S. Lewis, C.A. Barnes, M.J. Heben, A. Kumar, S.R. Lunt, G.E. McManis, G.M. Miskelly, R.M. Penner, M.J. Sailor, P.G. Santangelo, G.A. Shreve, B.J. Tufts, M.G. Youngquist, R.W. Kavanagh, S.E. Kellogg, R.B. Vogelaar, T.R. Wang, R. Kondrat and R. New, *Nature (London)*, 340 (1989) 525.
- 3 M.H. Salamon, M.E. Wrenn, H.E. Bergeson, K.C. Crawford, W.H. Delaney, C.L. Henderson, Y.Q. Li, J.A. Rusho, G.M. Sandquist and S.M. Seltzer, *Nature (London)*, 344 (1990) 401.
- 4 Proc. 1st Annu. Conf. on Cold Fusion, Salt Lake City, UT, 28–31 March 1990, National Cold Fusion Institute, Utah, August 1990.
- 5 AIP Conf. Proc. 228 on Anomalous Nuclear Effects in Deuterium/Solid Systems, Provo, UT, 22–24 October 1990, S.E. Jones, F. Scaramuzzi and D.H. Worledge (Eds.), American Institute of Physics, New York, 1991.
- 6 Special Symposium Proc. “Cold Fusion”, World Hydrogen Energy Conf. 8, Honolulu, HI, 22–27 July 1990, Hawaii Natural Energy Institute, HI, 1990.
- 7 M. Srinivasan, *Curr. Sci.*, 25 April 1991.
- 8 E.K. Storms, *Fusion Technol.*, in press.
- 9 P.L. Levine and K.E. Weale, *J. Chem. Soc. Faraday Trans.*, 56 (1960) 357.
- 10 C.M. Luedecke, G. Deublein and R.A. Huggins, in T.N. Veziroglu and J.B. Taylor (Eds.), *Hydrogen Energy Progress V*, Pergamon Press, New York, 1984, p. 1421.
- 11 C.M. Luedecke, G. Deublein and R.A. Huggins, *J. Electrochem. Soc.*, 132 (1985) 52.
- 12 B.Y. Liaw, G. Deublein and R.A. Huggins, presented at 6th Int. Solid State Ionics Conf., Garmisch-Partenkirchen, September 1987.
- 13 B.Y. Liaw, Ph.D. Dissertation, Stanford University, 1988.
- 14 G. Deublein and R.A. Huggins, *J. Electrochem. Soc.*, 136 (1989) 2234.
- 15 G. Alefeld and J. Vökel (Eds.), *Topics in Applied Physics*, Vols. 28, 29, *Hydrogen in Metals I, II*, Springer-Verlag, Berlin, 1978.
- 16 L. Schlapbach (Ed.), *Topics in Applied Physics*, Vol. 63, *Hydrogen in Intermetallic Compounds I*, Springer-Verlag, Berlin, 1988.
- 17 G. Deublein, B.Y. Liaw and R.A. Huggins, *Solid State Ionics*, 28/30 (1988) 1078.
- 18 G. Deublein, B.Y. Liaw and R.A. Huggins, *Solid State Ionics*, 28/30 (1988) 1084.
- 19 G. Deublein, B.Y. Liaw and R.A. Huggins, *Solid State Ionics*, 28/30 (1988) 1660.
- 20 S.-W. Chen, C.-H. Jan, J.-C. Lin and Y.A. Chang, *Metall. Trans. A*, 20 (1989) 2247.
- 21 I. Barin, O. Knaacke and O. Kubaschewski, *Thermochemical Properties of Inorganic Substances*, Springer-Verlag, Berlin, 1973; Supplement, 1977.
- 22 N.P. Yao, L.A. Herédy and R.C. Saunders, *J. Electrochem. Soc.*, 118 (1971) 1039.
- 23 C.J. Wen, B.A. Boukamp, R.A. Huggins and W. Weppner, *J. Electrochem. Soc.*, 126 (1979) 2258.
- 24 B.Y. Liaw, P.-L. Tao, P. Turner, B.E. Liebert and N.J. Hoffman, submitted to *Fusion Technol.*
- 25 B.F. Bush, J.J. Lagowski, M.H. Miles and G.S. Ostrom, *J. Electroanal. Chem.*, 304 (1991) 271.
- 26 B.Y. Liaw, P.-L. Tao and B.E. Liebert, Proc. 2nd Annu. Conf. on Cold Fusion, Conio, Italy 29 June–4 July 1991, T. Bressani, E. Del Giudice and G. Preparata (Eds.), Italian Physical Society, in press.